

Cite this: *Nanoscale*, 2012, **4**, 5627www.rsc.org/nanoscale

PAPER

Alumoxane/ferroxane nanoparticles for the removal of viral pathogens: the importance of surface functionality to nanoparticle activity†‡

Samuel J. Maguire-Boyle,^{ab} Michael V. Liga,^{ac} Qilin Li^{*ac} and Andrew R. Barron^{*abde}

Received 6th May 2012, Accepted 4th July 2012

DOI: 10.1039/c2nr31117h

A bi-functional nano-composite coating has been created on a porous Nomex® fabric support as a trap for aspirated virus contaminated water. Nomex® fabric was successively dip-coated in solutions containing cysteic acid functionalized alumina (alumoxane) nanoparticles and cysteic acid functionalized iron oxide (ferroxane) nanoparticles to form a nanoparticle coated Nomex® (NPN) fabric. From SEM and EDX the nanoparticle coating of the Nomex® fibers is uniform, continuous, and conformal. The NPN was used as a filter for aspirated bacteriophage MS2 viruses using end-on filtration. All measurements were repeated to give statistical reliability. The NPN fabrics show a large decrease as compared to Nomex® alone or alumoxane coated Nomex®. An increase in the ferroxane content results in an equivalent increase in virus retention. This suggests that it is the ferroxane that has an active role in deactivating and/or binding the virus. Heating the NPN to 160 °C results in the loss of cysteic acid functional groups (without loss of the iron nanoparticle's core structure) and the resulting fabric behaves similar to that of untreated Nomex®, showing that the surface functionalization of the nanoparticles is vital for the surface collapse of aspirated water droplets and the absorption and immobilization of the MS2 viruses. Thus, for virus immobilization, it is not sufficient to have iron oxide nanoparticles *per se*, but the surface functionality of a nanoparticle is vitally important in ensuring efficacy.

Introduction

Contamination of water by viral pathogens is endemic in many parts of the world. Sources of contamination include industrial and agricultural wastes, sewage and other forms of pollution. Sewage levels of approximately 7000 viruses per liter are common and can be more than 500 000 virus particles per liter.¹ Inhalation of this aspirated water can lead to serious infections and intoxications through exposure of mucous membranes in the eyes (conjunctiva), nose (rhinal) and mouth. In many cases gastroenteritis, respiratory disease, or eye, ear and nose infections result. However, more serious consequences and life-

threatening complications can occur. To overcome this, a viral filter for aspirated viruses would be of great utility.

The use of iron oxide nanoparticles as a component of a filter is reasonable since iron oxide and oxyhydroxides human toxicity is low,² and it has also been shown that Fe(O)OH and Fe₂O₃ are more resistant to acidic, corrosive, and oxidant conditions than other anti-viral materials (*e.g.*, silver).³ Most importantly, the affinity for binding of iron nanoparticles to virus pathogens has been observed in nature,⁴ where it has been shown that viruses interact and act as nucleation sites for the adsorption and precipitation of dissolved metals especially iron.⁵ Up to 50% of “dissolved iron” in sea water is between 30 nm and 100 nm in diameter.^{6–8} Between 90% and 99% of iron particulates are strongly chelated by organic ligands.^{7,8} Viral-lepidocrocite binding has been observed in sea water systems. Since virus adsorption is a function of surface area as well as surface activity, nanoparticles should show enhanced performance. However, an important question to answer is whether any such performance is simply a function of the “nano” nature of the iron oxide nanoparticle or a consequence of the surface functionality in concert with the nanoscale. The present research is aimed at understanding how the surface functionality of a nanoparticle can alter the efficacy of the nanoparticle activity.

Despite the efficacy of iron oxides and the potential of nano-crystalline iron oxides, there is a second important component of

^aRichard E Smalley Institute for Nanoscale Science and Technology, Rice University, Houston, Texas 77005, USA. E-mail: arb@rice.edu; qilin.li@rice.edu; Tel: +1-713-348-5610

^bDepartment of Chemistry, Rice University, Houston, Texas 77005, USA

^cDepartment of Civil and Environmental Engineering, Rice University, Houston, Texas 77005, USA

^dDepartment of Mechanical Engineering and Materials Science, Rice University, Houston, Texas 77005, USA

^eCollege of Engineering, Swansea University, Singleton Park, Swansea SA2 8PP, Wales UK

† Financial support for this work was provided by the US Navy and the Robert A. Welch Foundation (C-0002).

‡ Electronic supplementary information (ESI) available: SEM, EDX, and TEM images, XPS spectra, apparatus, and TGA/DTA. See DOI: 10.1039/c2nr31117h

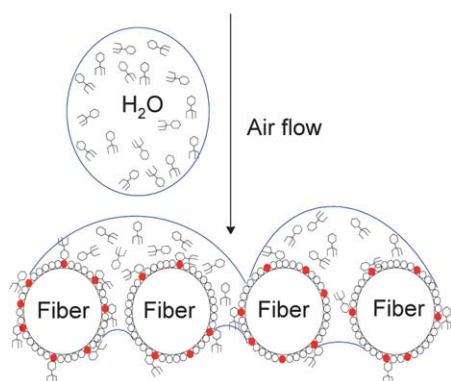


Fig. 1 Schematic diagram of an alumoxane/ferroxane viral trap showing the collapsed water droplet containing the virus on the fibers coated with both ferroxane (iron oxide) nanoparticles (dark circle) and alumoxane (alumina) nanoparticles (open circles).

any trap for aspirated viruses; it is necessary to provide a surface onto which water droplets will collapse. We have previously shown that coating a fabric with cysteic acid [$\text{HO}_2\text{CCH}(\text{NH}_2)\text{CH}_2\text{SO}_3\text{H}$] functionalized alumina nanoparticles (cysteic-alumoxane) results in a superhydrophilic surface that allows for the passage of water,⁹ but not hydrocarbons. In the present application, the function of the superhydrophilic surface as measured by an extremely low contact angle ($<3^\circ$) is to “collapse” airborne water droplets onto the surface, if this hydrophilic surface is combined with functionalization to trap and immobilize viruses then a combined system for removal of airborne or aspirated viruses may be achieved (Fig. 1). As noted above binding efficiency of iron oxides for viruses has been well documented suggesting that an iron oxide containing surface should be ideal as the trap. Thus, we propose that the creation of a bi-functional nano-composite coating on a porous support should provide a suitable test bed as a trap for aspirated virus contaminated water. The cysteic acid functionalized nanoparticles (alumina or iron oxide) should both cause the collapse of the water droplets, while the greater the iron content should trap and immobilize higher concentrations of viruses. Nomex® fabric was chosen as a convenient nanoparticle scaffold because of the uniformity of the fibers (providing a homogeneous support) and the large weave of the fabric (sufficient to allow viruses to pass through). In addition, its use in protective garments in hazardous locations¹⁰ and its tolerance to harsh conditions¹¹ make it a suitable practical substrate.

We have shown previously that carboxylic acid functionalized iron oxide nanoparticles (ferroxanes) are readily prepared from rust-like materials and propose the combination of hydrophilic surface alumoxane nanoparticles and viral binding functionalization ferroxane nanoparticles should make an effective hybrid material.¹²

Experimental section

1. Materials and methods

Cysteic acid, $\text{FeCl}_2 \cdot 4\text{H}_2\text{O}$, EtOH and acetone (Sigma-Aldrich) were used as received. Pseudoboehmite Catapal B was provided by Sasol North America Inc. Nomex® fabric was obtained from

Pegasus Auto Racing Supplies and was washed sequentially with EtOH and acetone to remove excess dye molecules. Energy dispersive spectroscopy (EDS) studies were performed on a FEI Quanta 400 ESEM. The samples were attached to a metal mount using carbon tape. Thermogravimetric/differential thermal analyses (TG/DTA) were obtained on a Q-600 Simultaneous TGA/DSC TA Instruments machine using a carrier gas of either dry argon or air. Scanning electron microscopy (SEM) studies were performed on a FEI Quanta 400 ESEM. A 5 nm layer of gold was sputtered onto the samples to provide a conducting surface. The samples were mounted on carbon tape. Transition electron microscopy (TEM) studies were performed on a JEOL 1230 HC-TEM 120 kV. Dilute solutions of nanoparticles were sonicated in DI water and drop cast onto 300 mesh copper grids the excess solution being wicked away. Samples containing MS2 were subsequently stained with 2% uranyl acetate (SPI-CHEM). The grids were received from Ted Pella with amorphous carbon surface and with the Formvar coating being removed by immersion of the grid in chloroform for thirty seconds and air drying just before drop casting. XPS studies were conducted on a PHI Quantera XPS machine. Samples were mounted onto the platen using double-sided carbon tape. Atomic force microscopy (AFM) measurements were conducted on a multimode AFM in tapping mode. The microscope was equipped with a Nanoscope IIIa scanning probe microscope controller and an Optizoom microscope from Digital Instruments. AFM tips were from K-TEK nanotechnology, which were the SPM probe model: TETA/Au (15) with an Au conductive coating and a resonant frequency of 300 Hz.

Bacteriophage MS2 (ATCC 15597-B1) and the host bacteria, *E. coli*, (ATCC 15597) were originally obtained from the ATCC, LB-Lennox media and sodium bicarbonate were purchased from Fisher Scientific, and Bacto™ agar was purchased from Difco Laboratories. Ultrapure water was obtained from a Barnstead E-Pure system. All materials were sterilized by autoclave, 70% EtOH, or filtration through a 0.22 μm membrane. Bacteriophage MS2 was used as a surrogate pathogenic virus in this study and was propagated using *E. coli* in LB-Lennox media (Fisher Scientific). 200 μL of MS2 stock solution was combined with 800 μL of an incubation of *E. coli*. This was combined with 3 mL of molten (45 $^\circ\text{C}$) LB-Lennox media containing 0.7% Bacto™ Agar (Difco Laboratories) and poured onto a Petri dish containing solid LB-Lennox media with 1.5% Bacto™ Agar. The plates were incubated overnight and subsequently filled with 15 mL of 100 mM NaHCO_3 solution (Fisher Scientific) and gently rocked for 3 hours.¹³ The buffer was withdrawn, centrifuged at $10\,900 \times g$ for 15 minutes, and the supernatant was passed through a 0.22 μm -pore-size syringe filter. The measured virus solution contained $\sim 7 \times 10^9$ PFU mL^{-1} and was stored at 4 $^\circ\text{C}$ until use in the virus removal experiments.

2. Synthesis

2.1. Synthesis of cysteic acid alumoxane nanoparticles. In a modification of the literature procedure,¹⁴ pseudoboehmite (100 g) was vigorously stirred in DI H_2O (80 mL), and to this was slowly added an aqueous 1 M solution of cysteic acid (80 mL). The resulting solution was allowed to stir overnight and then centrifuged at 4500 rpm for 1 h. The supernatant was evaporated

under vacuum and the resulting solid was used for coatings. Ceramic yield: 55%. Average particle size: 18 nm.

2.2. Synthesis of cysteic acid ferroxane nanoparticles. In a modification of the literature procedure,¹² a 1 M solution $\text{FeCl}_2 \cdot 4\text{H}_2\text{O}$ (100 mL) was mixed with 1.67 M solution of NaOH (100 mL). The ratio $R = [\text{FeCl}_2 \cdot 4\text{H}_2\text{O}]/[\text{NaOH}] = 0.6$ favors the formation of a pure lepidocrocite. To this was slowly added an aqueous 1 M solution of cysteic acid (80 mL). The resulting suspension was centrifuged at 4400 rpm for 30 min and the volatiles were removed in a vacuum at 90 °C. The resulting solid was used for subsequent coating experiments. Ceramic yield: 30%. Average particle size: 100 nm.

2.3. Formation of alumoxane/ferroxane hybrid material. A sample of Nomex® fabric (18 mL) was washed sequentially with EtOH and acetone to remove excess dye molecules. The fabric was then vacuum dried to remove all volatiles. The fabric was dip-coated in an aqueous solution of L-cysteic acid–alumoxane 20 wt% (10 g in 50 mL) and held there for 2–5 s. The dip-coat was allowed to oven dry (100 °C) before repeating the procedure three times. Loading of 5 wt% L-cysteic acid functionalized ferroxane (1.0 g in 20 mL DI H_2O) onto the L-cysteic acid alumoxane coated Nomex® resulted in the nanoparticle coated Nomex® (NPN) fabric, which was tested against aspirated MS2 bacteriophage for virus filtration. In order to limit potential nanoparticle shedding a similar sample was annealed to partially convert the nanoparticles to ceramic by heating the filter to 160 °C for 2 h in an argon atmosphere (NPN-160). Increased loading of 20 wt% cysteic ferroxane (5.0 g in 20 mL) was undertaken onto an alumoxane functionalized 18 cm^2 piece of Nomex® fabric (NPN-4x). The above membranes were characterized *via* XPS, SEM-EDS and tested as virus filter against MS2 bacteriophage.

3. Viral adsorption studies

The virus filtration experiments were conducted by generating an aerosolized virus stream, passing the output through a Nomex® fabric composite membrane the synthesis of which is outlined above, and collecting and enumerating the viruses that are

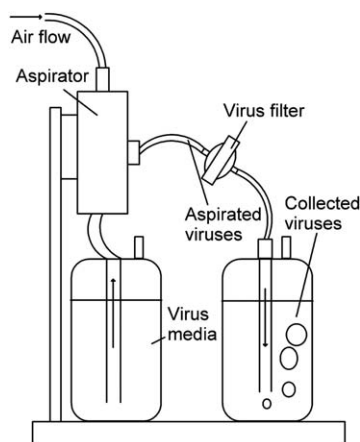


Fig. 2 Schematic diagram of the viral adsorption apparatus.

completely transported through the system (Fig. 2 and S1†). The aerosolized virus stream was generated using a TSI Constant Output Atomizer (model 3076, Shoreview, MN) operating in recirculation mode. The system was sterilized by operating with 70% EtOH followed by rinsing and operation with sterile ultrapure water prior to each experiment. To conduct an experiment, the virus stock was combined with 300 mL ultrapure water (final titer $\sim 10^6$ PFU mL^{-1}) in the feed reservoir, which was placed in an ice bath and connected to the atomizer. A 25 mm diameter piece of fabric was cut and placed in a reusable Swinnex® filter holder (Millipore, Billerica, MA) which was then attached to the discharge of the atomizer. The output of the filter holder was connected to a tube, which discharged through a stone diffuser into 150 mL of ultrapure water in a tall glass jar. The discharge water was sampled before each test and every 10 minutes up to 1 hour. Viruses in the samples were enumerated by the agar overlay method.¹⁵

Results and discussion

The strategy of our filters was to immobilize the nanoparticles onto a porous fabric scaffold (Fig. 1). To accomplish this, a fabric support with hydrophilic alumoxane and hydrophilic ferroxane nanoparticles was functionalized and subjected this filter to viral screening. Reduction in the concentration of viruses passing through the functionalized filter compared to the unfunctionalized filter was on the orders of magnitude.

Our previous work has shown that carboxylic acid functionalization of alumina surfaces can change the surface properties of the alumina.⁹ We have previously undertaken the study of many carboxylic acid functionalized hydrophilic surfaces. These effects were related to the hydrophilicity, as indicated by the contact angle of water on the surface. It was observed that cysteic acid functionalized alumina coated wafers were extremely hydrophilic, achieving complete wettability when in contact with water.⁹ In fact the extent of wetting is such that complete wetting of the surface results, which is attributed to the hydrogen bonding abilities of both sulfonyl and amine moieties, on functionalized cysteic acid and its zwitter ionic form (Fig. 3). Based on these results cysteic acid was chosen as the best candidate for the creation of our highly hydrophilic alumoxane–ferroxane Nomex® composite membrane.

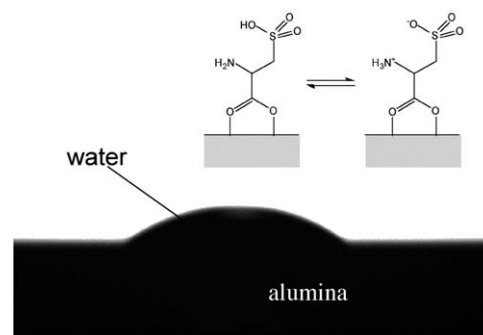


Fig. 3 Photographic image of water droplet on the cysteic acid functionalized alumina surface taken immediately upon dropping on the surface since within a few seconds the droplet completely wets the surface. The zwitter ionic forms of the cysteic acid are shown in the inset.

We have previously reported that carboxylic acid functionalized alumina and lepidocrocite nanoparticles (carboxylate alumoxanes and ferroxane) can be used to coat a range of fabrics and fibers.¹⁶ In the present case our goal was to deposit a thin layer of cysteic acid alumoxane onto a suitable support, anneal to 100 °C to provide a cysteic acid functionalized alumina surface on the support. Then repeat the process with ferroxane. TG/DTA analysis of the ferroxane nanoparticles (Fig. S4†) shows that heating to 100 °C results in loss of adsorbed water without loss of the cysteic acid functional groups.

In contrast to our previous membrane work,¹⁷ the resulting nanoparticle coated fabric (NPN) surface is not designed to act as a membrane on its own, but to be the sidewalls of a particle filtration membrane (10^3 to 10^6 nm pore size). SEM images indicated that deposition of the hydrophilic alumoxane and the viral active ferroxane nanoparticle occurred evenly across the fibers (Fig. 4). This observation is confirmed by EDS mapping of individual fibers (Fig. 5) showing a continuously uniformly coated single fiber as demonstrated by the overlap of the aluminum and iron EDS maps (Fig. 5b and c) with the SEM image of a fiber (Fig. 5a). The lower intensity of the iron signal is consistent with the lower concentration of the ferroxane. It is also important to note that the nitrogen and sulfur EDS maps (Fig. 5d and e) are identical since the sulfur is due to the cysteic acid functional group, while the nitrogen is due to both the cysteic acid functional group and the Nomex® aramid structure. If there were areas of the fibers not coated then the sulfur and nitrogen maps would be expected to be dissimilar. Uniform layering allows for passages of air with deposition of water droplets containing the target virus. Furthermore, from Fig. 4, it

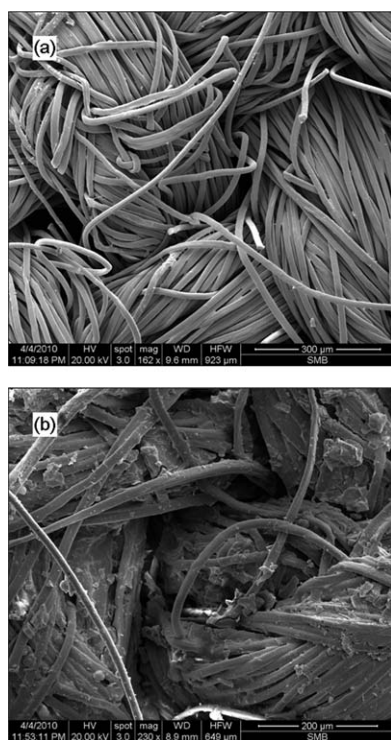


Fig. 4 SEM image of (a) uncoated Nomex fabric and (b) alumoxane/ferroxane composite coated fabric (NPN-2).

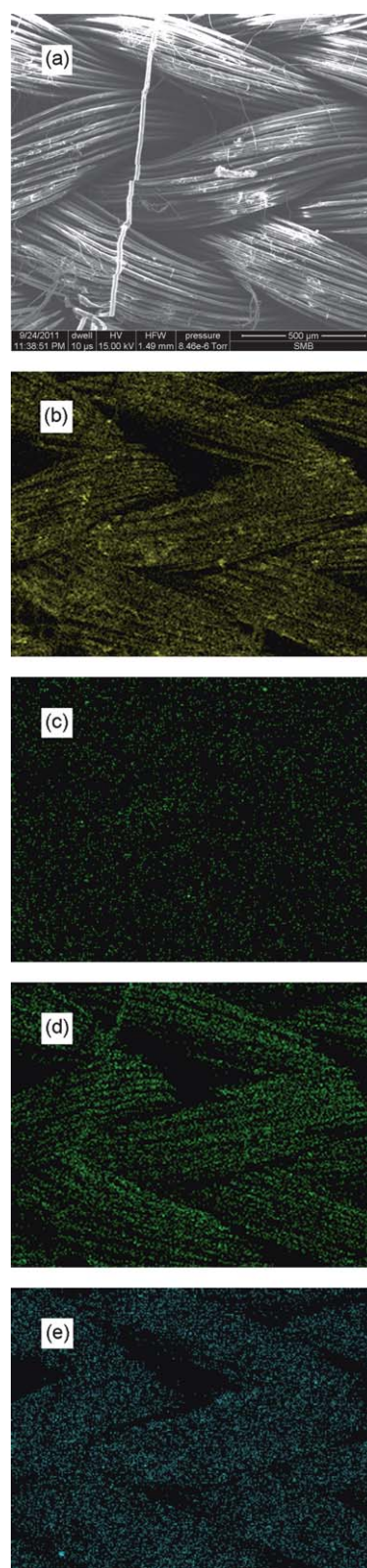


Fig. 5 SEM (a) and associated EDS maps of alumoxane/ferroxane nanoparticle coated fiber (NPN-2), (b) aluminum, (c) iron, (d) nitrogen, and (e) sulfur.

can be seen that there is no extensive webbing that would preclude flow through the filter or act such that the fabric pore sizes are decreased. This is confirmed by the observation that the

free flow of 2 kDa dextrans is not affected by the presence of the coating.⁹

The reason we chose to use Nomex® fabric as a support was that the large weave of the fabric cannot facilitate screening and thus it must be the surface of the fibers not pore size that is responsible for virus separation. Fabrication of the filter is achieved by first bringing the surface of the support into contact with a solution of cysteic acid functionalized alumoxane. The solution is drawn into the surface pores of the support by capillary forces. The surface coating thickness is controlled by the concentration of the cysteic acid alumoxane and ferroxane precursors and the pH of the solution. Size exclusion experiments using dextrans determined that the pore throat sizes of the functionalized membranes were sufficiently large as to not be an issue.⁹ Especially when considering that the Brownian motion of an aspirated water droplet as in its aerodynamic motion if less than 1 μm in diameter is significantly larger than its diameter.¹⁸ This ensures that in the application of our membrane for aspirated virus removal within an air-way the air flux is large while still ensuring capture of the aerosol water droplet.

Testing of virus filtration was undertaken using bacteriophage MS2; this is a single stranded (+)RNA virus with an icosahedral capsid about 25 nm in diameter.¹⁹ MS2 is similar to some water borne pathogenic viruses and has been used as a surrogate in several disinfection studies.²⁰ Compared to other bacteriophages, MS2 has been shown to be more resistant to UV disinfection.²¹ In disinfection studies using chlorine and chloramines, MS2 was found to be comparable or resistant compared to hepatitis A virus²² and poliovirus.²³ MS2 has also been recommended by the EPA as an indicator for viral inactivation processes.²⁴ MS2 is particularly convenient to work with, as its propagation and enumeration are relatively simple when compared to procedures required with pathogenic human viruses. The screening properties for MS2 of the functionalized membranes and unfunctionalized membranes were investigated, using end-on filtration of aspirated viruses. All virus trapping measurements were repeated to give statistical reliability.

Fig. 6 shows a plot of the cumulative number of viruses passing through each coated fabric as a function of time. It may clearly be seen that the alumoxane/ferroxane nanoparticle coated

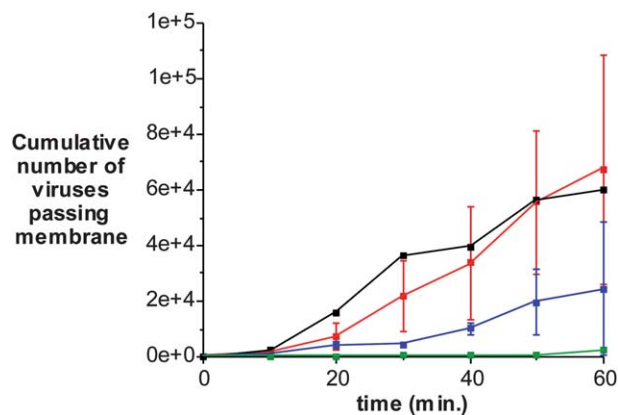


Fig. 6 Plot of a cumulative number of viruses passing through the Nomex®-derived filters as a function of exposure time for MS2 bacteriophage adsorption studies: untreated Nomex® (■), NPN (■), NPN-4x (■), and NPN heated to 160 °C for 2 hours (■).

fabrics (NPN and NPN-4x) show a large decrease as compared to Nomex® alone. A log plot is shown in Fig. S9.† It is particularly noteworthy that an increase in the ferroxane content (*i.e.*, sample NPN-4x *versus* sample NPN) results in an equivalent increase in virus retention. This suggests that it is the ferroxane that has an active role in either deactivating or binding to the virus. In order to confirm this result we have investigated the interaction of MS2 with individual ferroxane particles by TEM. Fig. 7a shows a TEM image of two MS2 viruses for comparison, while in the center of Fig. 7b is a representative example of a ferroxane particle to which is associated with multiple MS2 viruses (TEM images of ferroxane particles in the absence of MS2 are shown for comparison in Fig. S6†). In the entire TEM sample of NPN/MS2 all the ferroxane nanoparticles were observed “binding”, *i.e.*, being in close proximity to at least one if not multiple MS2 viruses.

From Fig. 6 it may be seen that the Nomex® fabric alone provides some barrier to transport aspirated MS2 bacteriophage in comparison to no fabric at all. This provides a simple measure of the physical barrier that any porous fabric would provide. Although previous work has suggested that iron oxides should act as efficient traps for viruses such as MS2, the coated fabric that was heated to 160 °C (NPN-160) shows essentially the same results as for untreated Nomex®, suggestive that the ferroxane is deactivated. However, TEM images of a sample of cysteic acid ferroxane heated to 160 °C which was then mixed in the presence of MS2 bacteriophage show particles associated with multiple MS2 viruses (Fig. 8) indicating that the binding of MS2 to the iron oxide nanoparticle is possible.

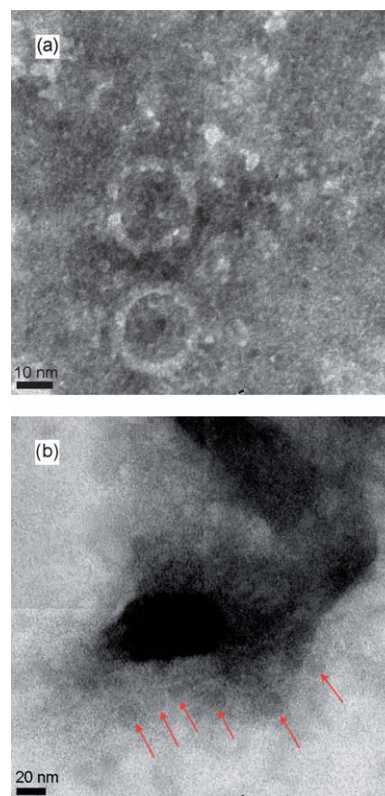


Fig. 7 TEM of (a) MS2 bacteriophage and (b) MS2 (arrowed) bound to cysteic acid-functionalized ferroxane nanoparticle.

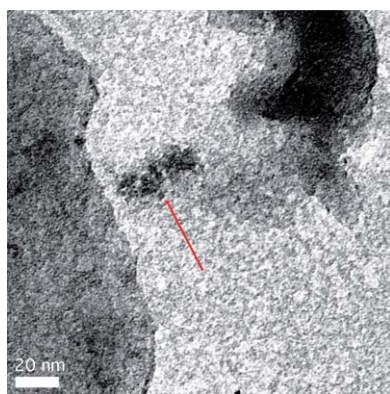


Fig. 8 TEM of MS2 bacteriophage (arrowed) bound to cysteic acid-functionalized ferroxane nanoparticle (left) that has been pretreated by heating to 160 °C for 2 hours.

These results are indicative of two issues. First, the nanoparticle coating process does not significantly alter the porosity of (or flow through) the fabric, since NPN-160 and Nomex® alone behave identically, and hence the results for NPN and NPN-4x are not a consequence of smaller pore/weave sizes. Second, TGA data indicate that annealing either cysteic acid alumoxane or ferroxane to 160 °C (Fig. S4†) results in the partial loss of functional groups on the nanoparticles without sintering of the individual nanoparticles and lowering the surface area.^{14,25} This suggests that the surface functionalization of the nanoparticles (*i.e.*, the hydrophilic surface due to the cysteic acid functional groups) is vital for the surface collapse of aspirated water droplet and the subsequent absorption and immobilization of the MS2 viruses. Thus we can conclude that a nanoparticle surface functionalization is far more important in the present process than the actual nanoparticle nature of the coating *per se*.

Conclusions

We have synthesized and characterized a permeable hydrophilic fabric-based filter with high flux for air flow and high virus binding capabilities, derived from simple hydrophilic principles and natural virus binding mechanisms found in nature. The benign nature of synthesis of the membrane composite ensures that future functionalization of any component within an airway system is possible with regards to virus inactivation. The concept of this membrane may be utilized in the future for functionalizing multiple components. While it is reasonable to propose that the ferroxane–MS2 interaction is essentially the same as in nature with regards to virus binding to lepidocrocite, the important result from this work is that it is not sufficient to have nanoparticles *per se*, but their surface functionality is important in ensuring functionality. In the present case this means the use of hydrophilic surface functionalization that ensures the collapse of aspirated water droplets and the wetting of the surface to allow exposure of the viruses to the “active” component of the surface.

Notes and references

- 1 W. Renate, W. Macht, J. Durkop, R. Hecht, U. Hornig and P. Schulze, *Water Res.*, 1989, **23**, 133–136.
- 2 R. M. Cornell and U. Schwertmann, *The Iron Oxides*, VCH, New York, 1996.
- 3 M. Pourbaix, *Atlas d'Equilibre Electrochimiques*, Gauthier-Villars, Paris, 1963.
- 4 C. J. Daughney, X. Chatellier, A. Chan, P. Kenward, D. Fortin, C. A. Suttle and D. A. Fowle, *Mar. Chem.*, 2004, **91**, 101–115.
- 5 L. A. Warren and F. G. Ferris, *Environ. Sci. Technol.*, 1998, **32**, 2331–2337; X. Chatellier, D. Fortin, M. M. West, G. G. Leppard and F. G. Ferris, *Eur. J. Mineral.*, 2001, **13**, 705–714; C. J. Daughney, D. A. Fowle and D. Fortin, *Geochim. Cosmochim. Acta*, 2001, **65**, 1025–1035; J. B. Fein, S. Scott and N. Rivera, *Chem. Geol.*, 2002, **182**, 265–273.
- 6 M. L. Wells and E. D. Goldberg, *Mar. Chem.*, 1992, **40**, 5–18; L. Wells and E. D. Goldberg, *Mar. Chem.*, 1993, **41**, 353–358; M. L. Wells and E. D. Goldberg, *Limnol. Oceanogr.*, 1994, **39**, 286–302.
- 7 J. Wu and G. W. Luther III, *Limnol. Oceanogr.*, 1994, **39**, 1119–1129; J. Wu and G. W. Luther III, *Mar. Chem.*, 1995, **50**, 159–177; J. Wu and G. W. Luther III, *Geochim. Cosmochim. Acta*, 1996, **60**, 2729–2741; J. Wu, E. Boyle, W. Sunda and L.-S. Wen, *Science*, 2001, **292**, 847–849.
- 8 J. Nishioka, S. Kakeda, C. S. Wong and W. K. Johnson, *Mar. Chem.*, 2001, **74**, 157–179.
- 9 S. J. Maguire-Boyle and A. R. Barron, *J. Membr. Sci.*, 2011, **382**, 107–115.
- 10 R. S. Villar, A. A. Martinez and J. M. D. Tascon, *J. Therm. Anal. Calorim.*, 2005, **79**, 529–532; L. T. Hasty, *Engineer*, 2003, **33**, 37; H. Gu, *Proc. Inst. Mech. Eng. S.*, 2009, **30**, 4324–4326.
- 11 Y. Sun and G. Sun, *Ind. Eng. Chem. Res.*, 2004, **43**, 5015–5020; A. Akdag, H. B. Kocer, S. D. Worley, R. M. Broughton, T. R. Webb and T. H. Bray, *J. Phys. Chem. B*, 2007, **111**, 5581–5586.
- 12 J. Rose, M. M. Cortalezzi-Fidalgo, S. Moustier, C. Magnetto, C. D. Jones, A. R. Barron, M. R. Wiesner and J.-Y. Bottero, *Chem. Mater.*, 2002, **14**, 621–628; M. M. Cortalezzi-Fidalgo, J. Rose, G. F. Wells, J.-Y. Bottero, A. R. Barron and M. R. Wiesner, *J. Membr. Sci.*, 2003, **227**, 207–217; J. Rose, M. R. Wiesner, and A. R. Barron, *US Pat.* 6,770,773, 2004.
- 13 M. Cho, H. Chung and J. Yoon, *Appl. Environ. Microbiol.*, 2005, **71**, 270–275.
- 14 R. L. Callender, C. J. Harlan, N. M. Shapiro, C. D. Jones, D. L. Callahan, M. R. Wiesner, D. B. MacQueen, R. Cook and A. R. Barron, *Chem. Mater.*, 1997, **9**, 2418–2433.
- 15 M. H. Adams, *Bacteriophages*, Interscience, New York, 1959.
- 16 R. L. Callender and A. R. Barron, *J. Mater. Sci.*, 2001, **36**, 4977–4987; R. L. Callender and A. R. Barron, *Ceram. Trans.*, 2000, **115**, 435–454; R. L. Callender and A. R. Barron, *J. Mater. Res.*, 2000, **15**, 2228–2237.
- 17 C. D. Jones, M. Fidalgo, M. R. Wiesner and A. R. Barron, *J. Membr. Sci.*, 2001, **193**, 175–184; D. A. Bailey, C. D. Jones, A. R. Barron and M. R. Wiesner, *J. Membr. Sci.*, 2000, **176**, 1–9; K. A. DeFriend, M. R. Wiesner and A. R. Barron, *J. Membr. Sci.*, 2003, **224**, 11–28; K. A. DeFriend and A. R. Barron, *J. Membr. Sci.*, 2003, **212**, 29–38.
- 18 S.-S. Lu, X. Wang, H. Hirano, T. Tagawa and H. Ozoe, *J. Appl. Phys.*, 2005, **98**, 114906–114909.
- 19 M. T. Madigan and J. M. Martinko, *Brock Biology of Microorganisms*, Pearson Prentice Hall, Upper Saddle River, NJ, 2006.
- 20 M. A. Butkus, *Appl. Environ. Microbiol.*, 2004, **70**, 2848–2853; Y. Koizumi and M. Taya, *Biochem. Eng. J.*, 2002, **12**, 107–116; E. D. Mackey, *J. - Am. Water Works Assoc.*, 2002, **94**, 62–69.
- 21 R. Sommer, *Water Res.*, 2001, **35**, 3109–3116.
- 22 M. D. Sobsey, T. Fuji and P. A. Shields, *Water Sci. Technol.*, 1988, **20**, 385–391.
- 23 J. A. Tree, M. R. Adams and D. N. Lees, *Appl. Environ. Microbiol.*, 2003, **69**, 2038–2043.
- 24 M. Pirnie, *Guidance Manual for Compliance with the Filtration and Disinfection Requirements for Public Water Systems Using Surface Water Sources*, USEPA, 1991.
- 25 R. L. Callender and A. R. Barron, *Adv. Mater.*, 2000, **12**, 734–738.